Electronic Supplementary Material (ESI) for Journal of Materials Chemistry A.

High-rate capability and energy density sodium ion full cell enabled by F-doped $Na_2Ti_3O_7$ hollow spheres

Du Pan[a,b,d], Weixin Chen[c], Shuwei Sun[a,b], Xia Lu[c], Xiaolei Wu[a,b], Caiyan Yu[a,b]*, Yong-Sheng Hu[d]*, Ying Bai[a,b]*

[a]International Joint Research Laboratory of New Energy Materials and Devices of Henan Province, School of Physics and Electronics, Henan University, Kaifeng, 475004, P. R. China.

[b]Academy for Advanced Interdisciplinary Studies Henan University, Kaifeng, 475004, P. R. China.

[c]School of Materials, Sun Yat-sen University, Guangzhou, 510006, P. R. China.

[d]Beijing National Laboratory for Condensed Matter Physics, Institute of Physics, Chinese Academy of Sciences, Beijing 100190, P. R. China.

E-mail: cyyu@henu.edu.cn (Caiyan Yu); yshu@iphy.ac.cn (Yong-Sheng Hu); ybai@henu.edu.cn (Ying Bai)

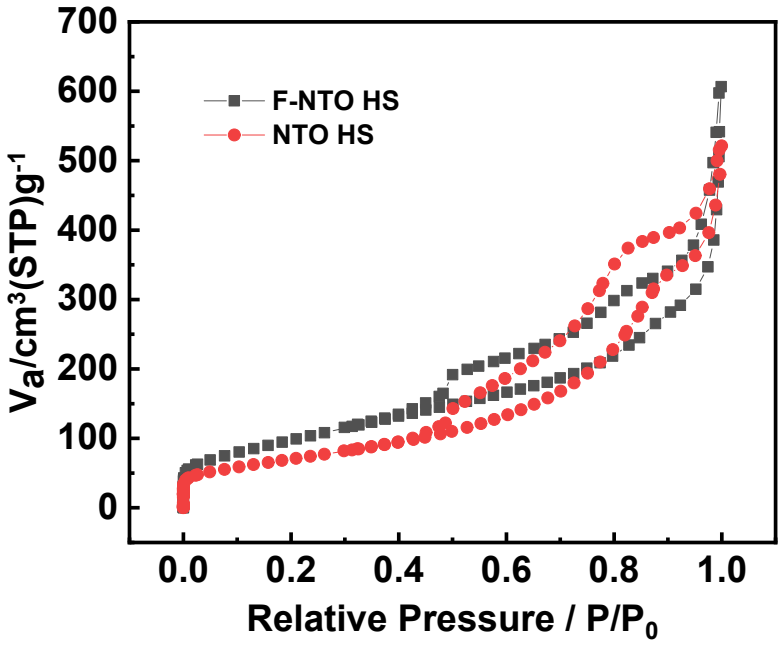

Fig. S1. N_2 adsorption isotherms distributions of the NTO HS and F-NTO HS samples.

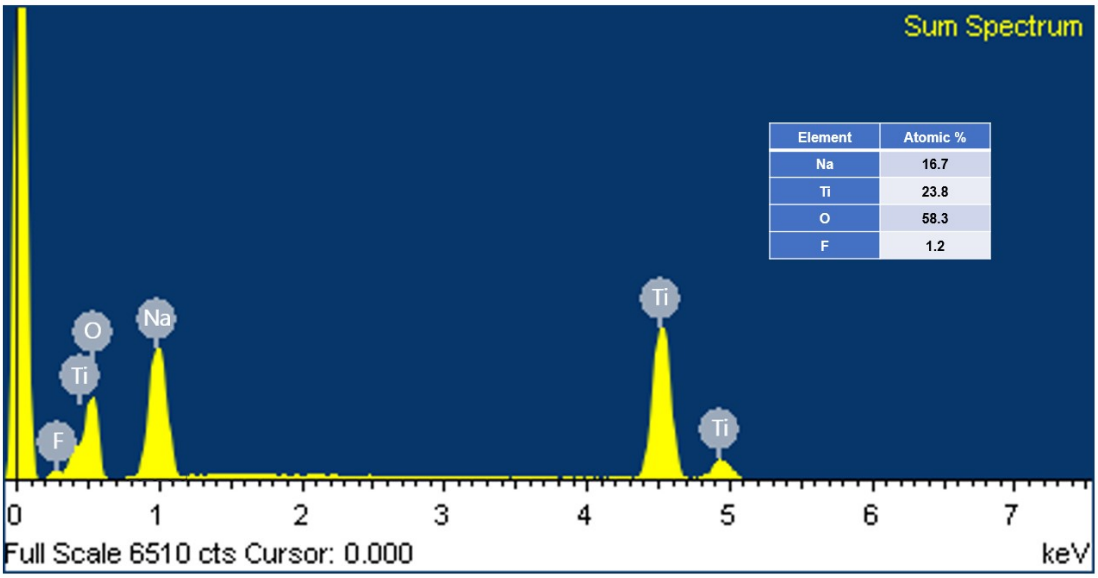

Fig. S2. EDS spectrum and corresponding element contents (inset) of F-NTO HS.

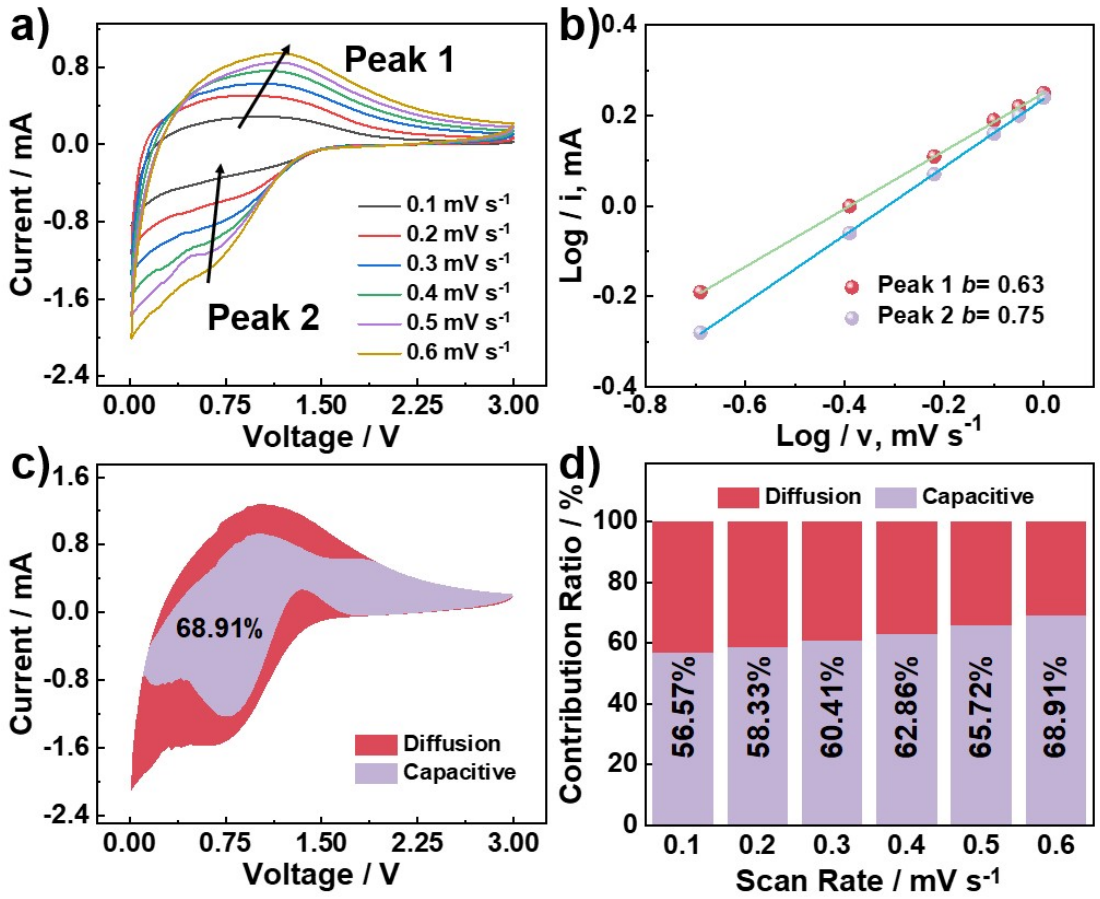

Fig. S3. CV curves collected under different scan rates (a). Regression relationship between log(scan rate) and log(peak current) (b). Capacitive and diffusion contributions of F-NTO HS at 0.6 mV s^{-1} (c). Normalized ratio of diffusion and capacitances under different scan rates (d).

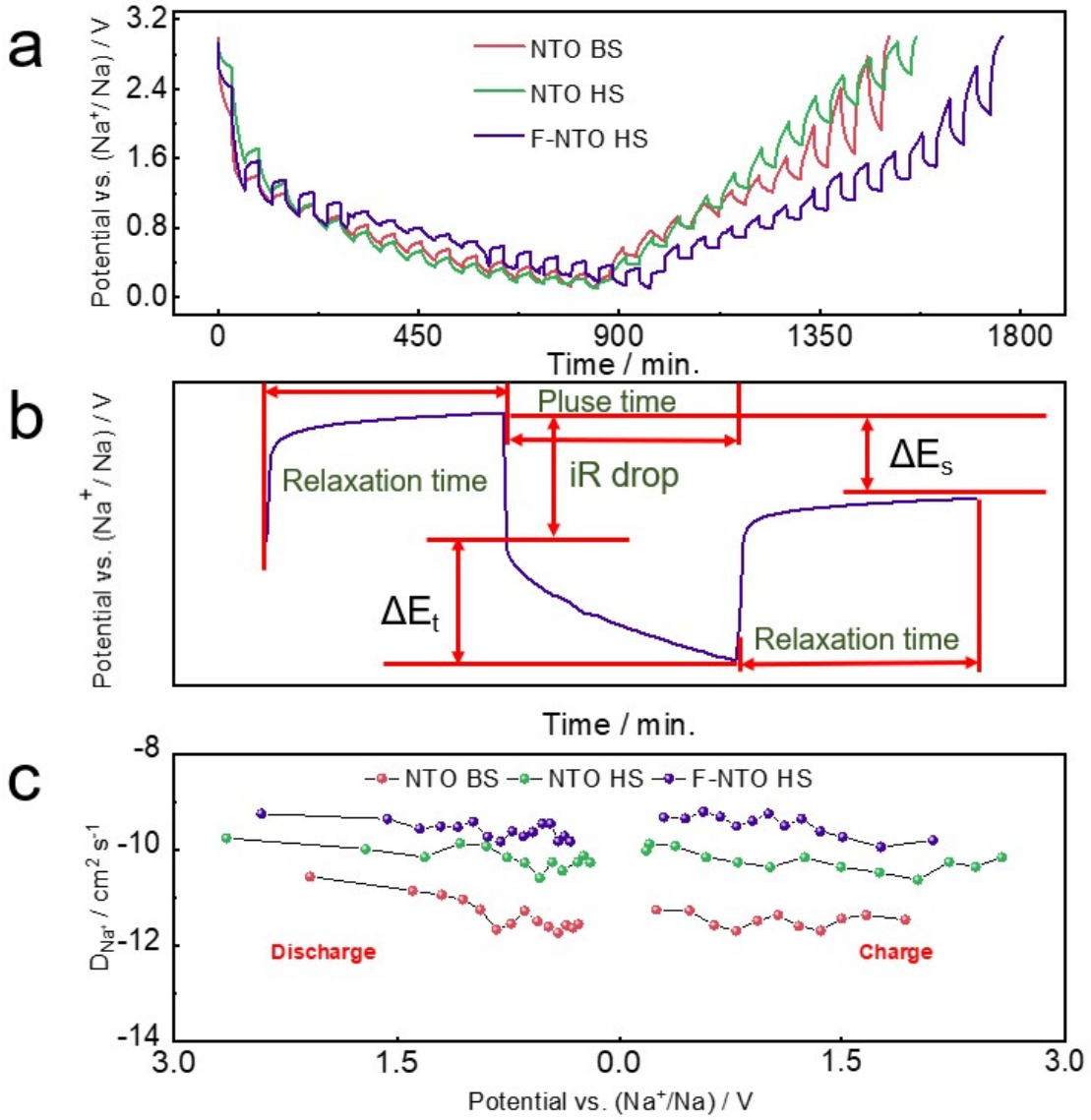

Fig. S4. Discharge-charge GITT curves after relaxation for 30 minutes at 0.1 A g^{-1} of NTO, NTO HS and F-NTO HS (a). E *versus* t profile of the F-NTO HS electrode for a single GITT during discharge process, which is composed of 30 *min.* galvanostatic charge (pluse) at 0.1 A g^{-1}, followed by 30 *min.* relaxation. The iR drop is shown along with the ΔE_τ and ΔE_s (b). The corresponding Na^+ diffusion coefficient (D_{Na^+}) (c).

The Na^+ diffusion coefficient can be obtained by the following equation:

$$D = \frac{4}{\pi\tau}\left(\frac{mV_m}{MA}\right)^2\left(\frac{\Delta E_s}{\Delta E_\tau}\right)^2 \quad (1)$$

Where τ is the relaxation time (s), m refers to the mass of active materials, A stands for

the geometric area of electrode. V_m and M mean the molar volume and molar mass of active materials, respectively. ΔE_s corresponds to quasi-thermodynamic equilibrium voltage change before and after the current pulse. ΔE_τ means the potential change during the current pulse.

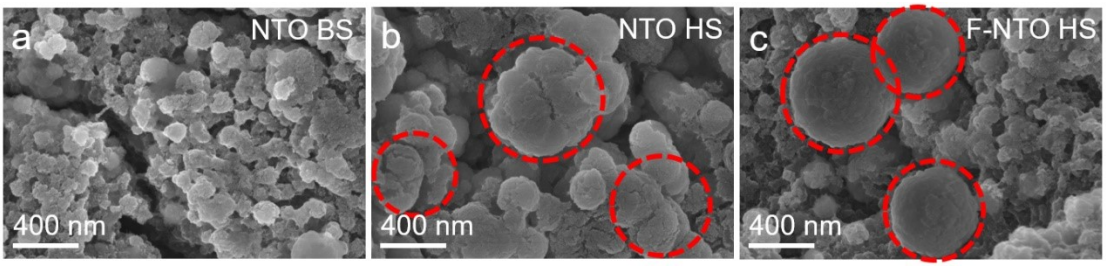

Fig. S5. SEM images of NTO HS (a), NTO HS (b) and F-NTO HS (c) anodes after 50 cycles.

Table S1. Electrochemical performances for the as-synthesized electrodes.

Performance		F-NTO HS	NTO HS	NTO BS
Rate capability / mAh g^{-1}	1C	281.3	233.5	154
	2C	237.2	197.3	125.8
	5C	201.1	170.0	111.8
	10C	180.2	155.4	103.4
	20C	166.3	145.8	82.6
	30C	155.5	135.9	71.8
	40C	145.5	122.4	64.7
	50C	135.6	115.3	60.8
Long-term cycling Stability / %	1000 cycles	67.5	44.3	24.9
	11000 cycles	87.29	47.13	0

Table S2. Electrochemical performance comparison of $Na_2Ti_3O_7$-based materials.[2-24]

material	Cycling capacity (mAh g^{-1})	Cycle number	current density (mA g^{-1})	Ref.
3D Microflowers NTO	100.1	1000	200	1
Hollow NTO	99.7	2000	5000	2
Red blood cell-like NTO@C	75.5	1000	3540	3
NTO@C	62.5	200	500	4
Layered NTO	131.4	1000	1000	5
3D NTO Nanosheet	135.5	1000	1000	6
NTO nanofibre	162.4	1000	708	7
NTO	42	90	1600	8
Layered NTO	181.5	100	600	9
NTO@C	187.2	100	177	10
N-NTO@C	88.9	1555	100	11
NTO@rGO	137.4	500	100	12
NTO	119.2	100	100	13

NTO Nanotube	84.5	10000	1770	14
NTO@C-BP	143.5	400	200	15
NTO	140.0	500	885	16
Double-Shell S-NTO	105.0	12000	8850	17
NTO nanotube/g-C_3N_4/ graphene	104.8	300	2000	18
NTO nanotube	60.5	500	400	19
Fe3O4@$Na_2Ti_3O_7$	172.4	1000	885	20
NTO@N-Doped Carbon	72.9	1000	8850	21
3D NTO	62.6	100	1000	22
This work	**138.8**	**11000**	**8850**	**/**

Table S3. Fitting Results of EIS Data for as-synthesized electrodes.

Cycle number	NTO HS		F-NTO HS	
	Rsf / Ω	D_{Na+} / $cm^2 s^{-1}$	Rsf / Ω	D_{Na+}/ $cm^2 s^{-1}$
1st	50.4	0.78×10^{-10}	42.3	1.88×10^{-10}
25th	132.5	0.40×10^{-10}	73.8	1.76×10^{-10}
50th	190.2	0.19×10^{-10}	108.4	1.82×10^{-10}
75th	290.4	0.11×10^{-10}	145.6	1.95×10^{-10}
100th	389.9	0.07×10^{-10}	176.7	1.81×10^{-10}

Table S4. Bader charge analysis of Ti.

ion	NO.	NTO			NTO-F		
		Charge/e$^-$	d_{min}/nm	Volume/Å^3	Charge/e$^-$	d_{min}/nm	Volume/Å^3
Ti	1	2.102393	0.800657	7.829199	2.190750	0.905757	8.102746
	2	2.102393	0.800657	7.829199	2.190750	0.905757	8.102746
	3	2.080788	0.842283	7.761505	2.187370	0.838958	8.094408
	4	2.080788	0.842283	7.761505	2.187370	0.838958	8.094408
	5	2.102394	0.800657	7.829199	2.120253	0.807463	7.949695
	6	2.102394	0.800657	7.829199	2.120253	0.807463	7.949695
	7	2.091610	0.816787	7.932239	2.099675	0.807544	8.039024
	8	2.091610	0.816787	7.932239	2.099675	0.807544	8.039024
	9	2.091610	0.816787	7.932239	2.104626	0.811921	7.950886
	10	2.091610	0.816787	7.932239	2.104626	0.811921	7.950886
	11	2.080788	0.842283	7.761505	2.085374	0.85661	7.765677
	12	2.080788	0.842283	7.761505	2.085374	0.85661	7.765677
TiO_2: +4		**～2.054**		**$NaTi_2O_4$: +3.5**	**～2.179**		**$NaTiO_2$: +3** **～2.340**

Table S5. Experimental and calculated diffusion coefficients for NTO and NTO-F

	Direction	Path	Sample	Energy barrier/eV	Diffusion coefficient /cm^2 s^{-1}	Sample	Energy barrier/eV	Diffusion coefficient /cm^2 s^{-1}
Exp.	-	-	NTO	-	1.09×10^{-1}	NTO-F	-	4.27×10^{-10}
	b	Path 1	NTO	0.24	1.56×10^{-7}	NTO-F	0.32	7.22×10^{-9}
		Path 2		-	-		0.33	4.91×10^{-9}
		Path 3		0.20	7.30×10^{-7}		0.25	1.07×10^{-7}
		Path 4		-	-		0.28	3.37×10^{-8}
Cal.	a	Path 1	NTO	2.4	1.30×10^{-35}	NTO-F	2.8	2.72×10^{-42}
	c	Path 1	NTO	0.49	1.04×10^{-11}	NTO-F	0.41	2.27×10^{-10}
		Path 2		0.31	1.07×10^{-8}		0.41	2.27×10^{-10}
		Path 3		0.26	7.26×10^{-8}		0.24	1.57×10^{-7}
		Path 4		0.17	2.31×10^{-6}		0.22	3.39×10^{-7}

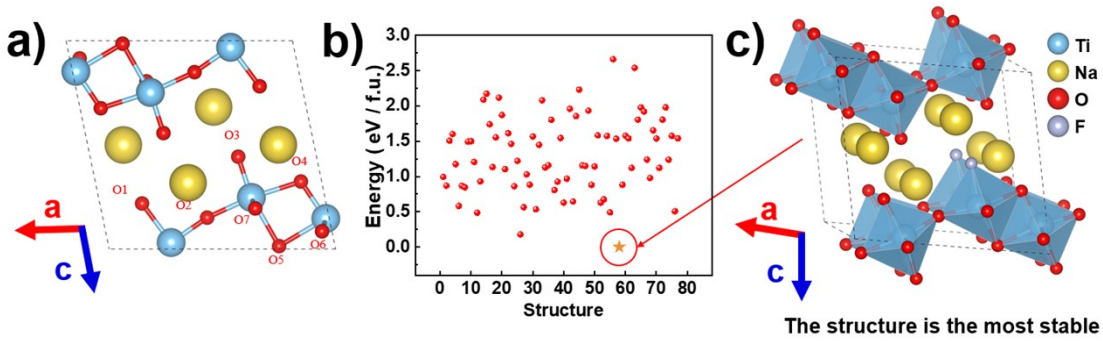

Fig. S6. Different sites of O in NTO-F (a). Energy of different configurations (b) and crystal structure of the most stable configuration for the NTO-F (c).

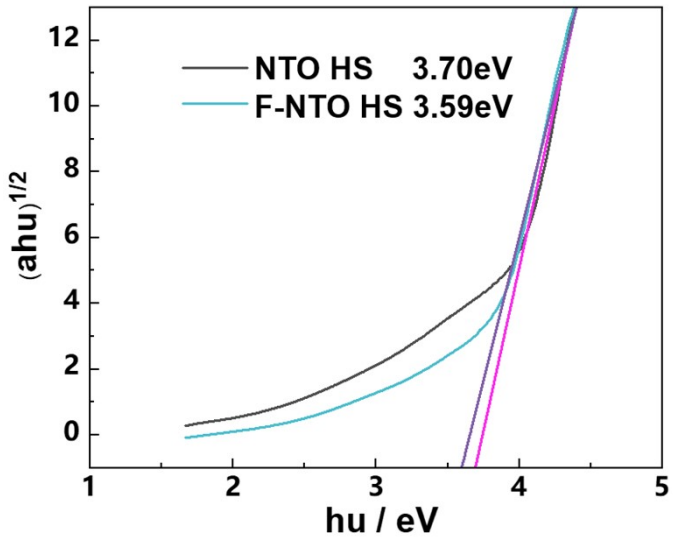

Fig. S7. Tauc plot of the NTO HS and F-NTO HS.

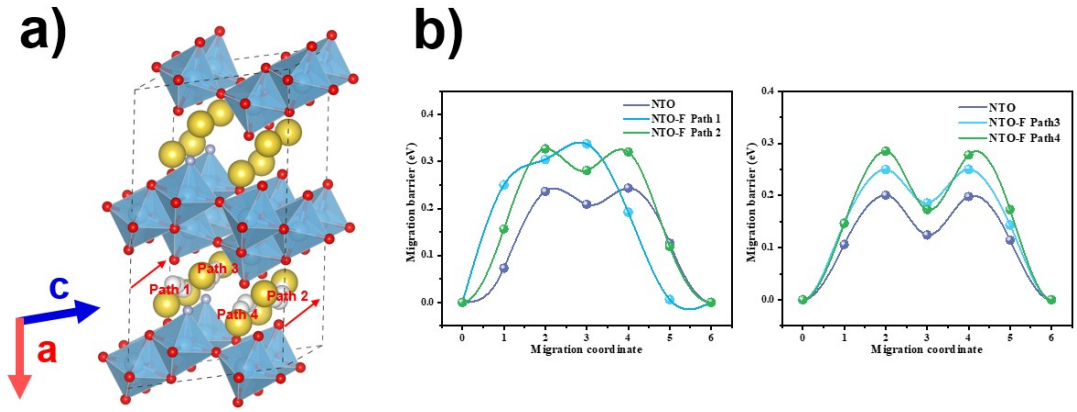

Fig. S8. The b-axis direction of NTO-F (a). Energy barriers of Na^+ for different diffusion paths (b).

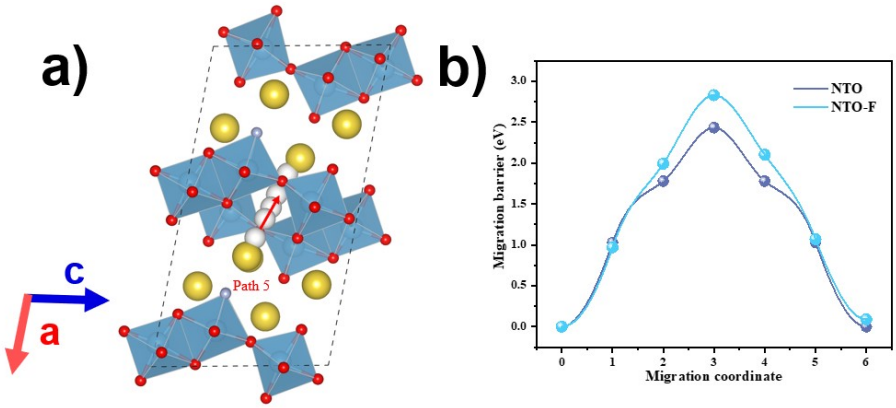

Fig. S9. The a-axis direction of NTO-F (a). Energy barriers of Na^+ for diffusion paths (b).

References

1 C.J. Wen, R.A. Huggins, *Mater. Res. Bull.*, 1980, **15**, 1225.

2 W. Weppner, *J. Electrochem. Soc.*, 1977, **124**, 1569.

3 S. Anwer, Y. Huang, J. Liu, J. Liu, M. Xu, Z. Wang, R. Chen, J. Zhang and F. Wu, *ACS Appl. Mater. Interfaces*, 2017, **9**, 11669-11677.

4 H. Chen, Y. Wu, J. Duan, R. Zhan, W. Wang, M.Q. Wang, Y. Chen, M. Xu and S.J. Bao, *ACS Appl. Mater. Interfaces*, 2019, **11**, 42197-42205.

5 S. Chen, Y. Pang, J. Liang and S. Ding, *J. Mater. Chem. A*, 2018, **6**, 13164-13170.

6 C. Ding, T. Nohira and R. Hagiwara, *J. Power Sources*, 2017, **354**, 10-15.

7 S. Dong, Z. Li, I.A. Rodríguez-Pérez, H. Jiang, J. Lu, X. Zhang and X. Ji, *Nano Energy*, 2017, **40**, 233-239.

8 S. Dong, L. Shen, H. Li, G. Pang, H. Dou and X. Zhang, *Adv. Funct. Mater.*, 2016, **26**, 3703-3710.

9 D. Kong, Y. Wang, S. Huang, Y.V. Lim, J. Zhang, L. Sun, B. Liu, T. Chen, P. Valdivia y Alvarado and H.Y. Yang, *J. Mater. Chem. A*, 2019, **7**, 12751-12762.

10 T.L. Kulova, Y.O. Kudryashova, A.A. Kuz'mina, A.M. Skundin, I.A. Stenina, A.A. Chekannikov, A.B. Yaroslavtsev and J. Libich, *J Solid State Electrochem.*, 2018, **23**, 455-463.

11 H. Li, L. Peng, Y. Zhu, D. Chen, X. Zhang and G. Yu, *Energy Environ. Sci.*, 2016, **9**, 3399-3405.

12 M. Li, X. Xiao, X. Fan, X. Huang, Y. Liu and L. Chen, *J. Alloys Compd.*, 2017, **712**, 365-372.

13 P. Li, W. Wang, S. Gong, F. Lv, H. Huang, M. Luo, Y. Yang, C. Yang, J. Zhou, C. Qian, B. Wang, Q. Wang and S. Guo, *ACS Appl. Mater. Interfaces*, 2018, **10**, 37974-37980.

14 Z. Li, Y. Huang, Y. Jiang, Z. Wang, B. Lu, J. Zhou and M. Xie, *ChemElectroChem*, 2020, **7**, 2258-2264.

15 A. Mukherjee, S. Mondal, D. Das, S. Banerjee and S.B. Majumder, *Mater. Lett.*, 2021, **301**, 130219.

16 J. Ni, S. Fu, C. Wu, Y. Zhao, J. Maier, Y. Yu and L. Li, *Adv. Energy Mater.*, 2016,

6, 1502568.

17 T. Song, H. Chen, Q. Xu, H. Liu, Y.G. Wang and Y. Xia, *ACS Appl. Mater. Interfaces*, 2018, **10**, 37163-37171.

18 D. Sriramulu and H.Y. Yang, *Nanoscale*, 2019, **11**, 5896-5908.

19 N. Wang, X. Xu, T. Liao, Y. Du, Z. Bai and S. Dou, *Adv. Mater.*, 2018, **30**, 1804157.

20 S. Wang, Y. Zhu, M. Jiang, J. Cui, Y. Zhang and W. He, *Int. J. Hydrog. Energy*, 2020, **45**, 19611-19619.

21 Y. Wu, J. Wu, S. Zhang, L. Zhu, Z. Yan and X. Cao, *J Solid State Chem*, 2021, **300**, 122247.

22 X. Wang, Y. Li, Y. Gao, Z. Wang and L. Chen, *Nano Energy*, 2015, **13**, 687-692.

23 F. Xie, L. Zhang, D. Su, M. Jaroniec and S.Z. Qiao, *Adv. Mater.*, 2017, **29**, 1700989.

24 Q. Zhang, T. Zhang, Y. Wei, T. Zhai and H. Li, *J. Mater. Chem. A*, 2017, **5**, 18691-18697.